International Journal of Astrobiology 16 (3): 203–217 (2017)
doi:10.1017/S1473550416000057

Measurements of Oxychlorine species on Mars

B. Sutter[1,2], R. C. Quinn[3], P. D. Archer[1,2], D. P. Glavin[4], T. D. Glotch[5], S. P. Kounaves[6], M. M. Osterloo[7], E. B. Rampe[2,8] and D. W. Ming[2]

[1]*Jacobs Technology, Houston, TX, USA e-mail: brad.sutter-2@nasa.gov*
[2]*NASA Johnson Space Center, Houston, TX, USA*
[3]*SETI Institute, NASA/Ames Research Center, Mountain View, CA, USA*
[4]*NASA Goddard Space Flight Center, Greenbelt, MD, USA*
[5]*Stony Brook University, Stony Brook, NY, USA*
[6]*Tufts University, Medford, MA, USA*
[7]*LASP, University of Colorado, Boulder, CO, USA*
[8]*Aerodyne Industries, Jacobs JETS, Houston, TX, USA*

Abstract: Mars landed and orbiter missions have instrumentation capable of detecting oxychlorine phases (e.g. perchlorate, chlorate) on the surface. Perchlorate (~0.6 wt%) was first detected by the Wet Chemistry Laboratory in the surface material at the Phoenix Mars Landing site. Subsequent analyses by the Thermal Evolved Gas Analyser aboard the same lander detected an oxygen release (~465°C) consistent with the thermal decomposition of perchlorate. Recent thermal analysis by the Mars Science Laboratory's Sample Analysis at Mars instrument has also indicated the presence of oxychlorine phases (up to 1.2 wt%) in Gale Crater materials. Despite being at detectable concentrations, the Chemistry and Mineralogy (CheMin) X-ray diffractometer has not detected oxychlorine phases. This suggests that Gale Crater oxychlorine may exist as poorly crystalline phases or that perchlorate/chlorate mixtures exist, so that individual oxychlorine concentrations are below CheMin detection limits (~1 wt%). Although not initially designed to detect oxychlorine phases, reinterpretation of Viking Gas Chromatography/Mass Spectrometer data also suggest that oxychlorine phases are present in the Viking surface materials. Remote near-infrared spectral analyses by the Compact Reconnaissance Imaging Spectrometer for Mars (CRISM) instrument indicate that at least some martian recurring slope lineae (RSL) have spectral signatures consistent with the presence of hydrated perchlorates or chlorates during the seasons when RSL are most extensive. Despite the thermal emission spectrometer, Thermal Emission Imaging System, Observatoire pour la Minéralogie, l'Eau, les Glaces et l'Activité and CRISM detection of hundreds of anhydrous chloride (~10–25 vol%) deposits, expected associated oxychlorine phases (>5–10 vol%) have not been detected. Total Cl and oxychlorine data sets from the Phoenix Lander and the Mars Science Laboratory missions could be used to develop oxychlorine versus total Cl correlations, which may constrain oxychlorine concentrations at other locations on Mars by using total Cl determined by other missions (e.g. Viking, Pathfinder, MER and Odyssey). Development of microfluidic or 'lab-on-a-chip' instrumentation has the potential to be the next generation analytical capability used to identify and quantify individual oxychlorine species on future landed robotic missions to Mars.

Received 19 August 2015, accepted 8 February 2016, first published online 5 April 2016

Key words: Perchlorate, chlorate, Mars, chlorine

Introduction

Perchlorate (ClO_4^-) was measured at the Mars Phoenix landing site using the Microscopy Electrochemistry and Conductivity Analyser Wet Chemistry Laboratory (WCL) (Hecht *et al*. 2009; Kounaves *et al*. 2010) and its presence, based on oxygen release, was also confirmed by the Phoenix Thermal Evolved Gas Analyser (Hecht *et al*. 2009). Based on the initial detection of perchlorate, spectral analysis using the Phoenix Surface Stereo Imager indicated a possible heterogeneous distribution of hydrated-perchlorate at the Phoenix landing site (Cull *et al*. 2010). Although in contrast, WCL data show a relatively uniform abundance in the samples analysed (Kounaves *et al*. 2010; Toner *et al*. 2014). Following the detection of perchlorate at the Phoenix site, a reanalysis of the Viking Gas Chromatography/Mass Spectroscopy (GCMS) data indicated the presence of oxychlorine phase like perchlorate at both Viking landing sites (Navarro-González *et al*. 2010). Results from the Sample Analysis at Mars (SAM) instrument suite on board the Curiosity rover suggest the presence of oxychlorine phases, likely perchlorate and chlorate (ClO_3^-), in Gale Crater (Glavin *et al*. 2013; Leshin *et al*. 2013; Archer *et al*. 2014; Ming *et al*; 2014; Freissinet *et al*. 2015). Remotely sensed infrared (IR) spectra acquired by the Compact Reconnaissance Imaging Spectrometer for Mars (CRISM) are consistent with hydrated-chlorate or hydrated-perchlorate in recurring slope lineae (RSL) features on Mars (Ojha *et al*. 2015). These hydrated features appear to only be present during the summer

Table 1. *Total chlorine, perchlorate (ClO_4^-) and chloride (Cl^-) detected on Mars as determined by surface and orbital instrumentation.*

Mission	Soil/sediment	Detection method	Total Cl	Cl^-	ClO_4^-
			(wt%)		
	Rocknest eolian deposit[a,b,c]	APXS	0.69 ± 0.03	–	–
		SAM-EGA	–	–	0.39 ± 0.06[n]
MSL	John Klein mudstone[d]	APXS	0.52 ± 0.02	–	–
		SAM-EGA	–	–	0.12 ± 0.02
	Cumberland mudstone[d]	APXS	1.19 ± 0.04	–	–
		SAM-EGA	–	–	1.08 ± 0.04
	Rosy red soil[e]	WCL	–	0.05 ± 0004	0.67 ± 007
Phoenix	Sorceress 1 Soil[e]	WCL	–	0.03 ± 0001	0.68 ± 005
	Sorceress 2 Soil[e]	WCL	–	0.04 ± 0001	0.62 ± 003
Mars Reconnaissance orbiter	Recurring Slope Lineae[f]	CRISM	–	–	Unknown
Mars odyssey	Chloride deposits[g,h]	THEMIS	–		–
Mars express	”	OMEGA	–	10–25	–
Mars global surveyor	”	TES	–	vol%	–
Mars odyssey	Global Cl[i]	GRS	0.2–0.8 ± <0.2	–	–
MER spirit	Gusev Soil[j,k]	APXS	0.54–0.94 ± <0.08	–	–
MER opportunity	Meridiani Soil[j,k]	APXS	0.41–0.77 ± <0.06	–	–
Pathfinder	Ares Vallis Soil[l]	APXS	0.55 ± 0.2	–	–
VL1	Chryse Planita Soil[m]	XRF	0.7–0.9 ± 0.5	–	–
VL2	Utopia Planita Soil[m]	XRF	0.3–0.6 ± 0.5	–	–

APXS, Alpha Particle X-ray Spectrometer; SAM-EGA, Sample Analysis at Mars Evolved Gas Analysis; WCL, Wet Chemistry Laboratory; XRF, X-ray Fluorescence; CRISM, Compact Reconnaissance Imaging Spectrometer for Mars; THEMIS, Thermal Emission Imaging System; OMEGA, Observatoire pour la Minéralogie, l'Eau, les Glaces et l'Activité; TES, Thermal Emission Spectrometer; GRS, Gamma Ray Spectrometer.
[a]Leshin *et al.* (2013); [b]Archer *et al.* (2014); [c]Blake *et al.* (2013); [d]Ming *et al.* (2014); [e]Fang *et al.* (2015); [f]Ojha *et al.* (2015); [g]Osterloo *et al.* (2008); [h]Jensen & Glotch (2011). [i]Keller *et al.* (2006); [j]Morris *et al.* (2006); [k]Yen *et al.* (2006); [l]Brückner *et al.* (2003); [m]Clark *et al.* (1982).
[n]Perchlorate concentration determined from evolved SAM–EGA O_2 results assuming that all oxygen is derived from perchlorate.

when the RSL are at their maximum spatial extent. Oxychlorine phase in this work refers to oxygen bearing Cl anions that fall into the series: hypochlorite (ClO^-), chlorite (ClO_2^-), chlorate (ClO_3^-) and perchlorate (ClO_4^-). Hypochlorite and chlorite are typically thought of as intermediate phases involved in chlorate and perchlorate formation (e.g. Catling *et al.* 2010; Carrier & Kounaves, 2015) and may not accumulate in martian materials to the same level as perchlorate or chlorate. However, hypochlorite and chlorite in martian surface materials cannot be ruled out; therefore, oxychlorine will be the term used to account for all possible oxygen bearing Cl phases that may be present on Mars.

The occurrence of oxychlorine phases at widely spaced locations on Mars (Phoenix Landing site, Gale Crater and RSL features) suggests that oxychlorine phases may occur throughout the martian surface. The measurement of high chlorine (e.g. Clark *et al.* 1977; Rieder *et al.* 1997; Rieder *et al.* 2004; Gellert *et al.* 2006; Keller *et al.* 2006; Blake *et al.* 2013; Gellert *et al.* 2013) (Table 1) and chloride (Osterloo *et al.* 2008) concentrations all over Mars by orbital and landed instrumentation suggests that oxychlorine could be a component of these other chlorine detections. This is supported by the fact that oxychlorine phases are a component of the total Cl detected at that Phoenix and Gale Crater landing sites. IR spectroscopy and X-ray diffraction (XRD) analysis of Mars surface materials are capable of detecting oxychlorine phases such as perchlorate and chlorate. These techniques may thus be useful for identifying oxychlorine phases in locations where chlorine or chloride has been detected. Furthermore, where oxychlorine and chlorine or chloride have been determined, such relationships may be useful in constraining oxychlorine concentrations where only total chlorine or chloride data are available.

The goal of this review is to evaluate analytical techniques employed to detect and measure oxychlorine phases on Mars. The specific objectives of this review are to: (1) Discuss oxychlorine detection techniques employed on landed and orbital missions and their limitations; (2) Evaluate oxychlorine versus total Cl determinations from the Phoenix and Mars science laboratory (MSL) missions and how this relationship could be used to constrain oxychlorine levels at other sites (e.g. Viking, Mars Pathfinder, Mars Exploration Rovers, Mars Odyssey Gamma Ray Spectrometer (GRS)); and (3) Briefly discuss alternative analytical technology for detecting oxychlorine phases on future missions to Mars.

Phoenix Lander WCL

The WCL onboard the Phoenix Lander conducted the first analysis of soluble ionic species in the martian soil and resulted in the first direct detection of perchlorate on the martian surface. A detailed description of the Phoenix-WCL has been previously published (Kounaves *et al.* 2009) and is only briefly reviewed here. The WCL was consisted of an upper 'actuator' and a lower 'beaker' assembly. The actuator consisted of a titanium container that held 25 ml of deionized water plus $\sim 10^{-5}$ M concentrations of selected ionic species for initial

https://doi.org/10.1017/S1473550416000057

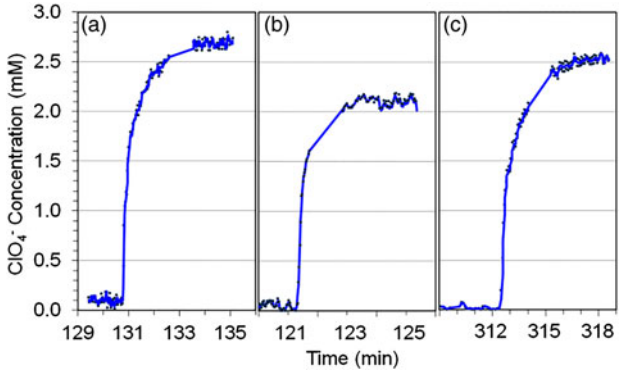

Fig. 1. Concentration of ClO_4^- in the WCL beaker solution after addition of ~1 cm^3 of soil to 25 ml of water for (a) Rosy Red on Sol-30, (b) Sorceress-1 on Sol-41 and (c). Sorceress-2 on Sol-107 samples. Solution concentrations are equivalent to 0.67, 0.68 and 0.62 wt% ClO_4^- in the soil, respectively. The wt% ClO_4^- for the Sorceress-1 sample has been adjusted to reflect the delivery of only 0.75 cc soil.

sensor calibrations; a drawer for accepting 1 cm^3 of soil through a screened funnel; a stirrer; and a reagent dispenser. The lower 'beaker' contained an array of sensors for determination of selected soluble ions, pH, and also solution properties such as electrical conductivity and redox potential (E_h).

Soil samples were successfully added and analysed in three of the four WCL cells, one from the surface on sol 30 (Rosy Red) and two from the top of the ice table ~5 cm in depth on sols 41 and 107 (Sorceress-1 and Sorceress-2). All three samples were found to contain ionic species similar to those generally measured on Earth, including mM levels in solution of Mg^{2+}, Ca^{2+}, Cl^-, Na^+, K^+ and $SO_4^=$, and a pH of ~7.7 (Kounaves *et al.* 2010). One ion-selective sensor in the WCL array, originally designated as a nitrate (NO_3^-) sensor, responds to a large number of anionic species with selectivity that follows the Hofmeister series ($ClO_4^- > I^- > SCN^- > ClO_3^- > CN^- > Br^- > BO_3^{3-} > NO_3^- > Cl^-$). The response of this sensor to ClO_4^- is three orders-of-magnitude greater than any other species. For all three WCL samples, a ~200 mV sensor response was observed (Fig. 1). The magnitude of this response exceeded the signal response limit, based on the sample size, for the possible concentrations of any other anionic species, with the exception of ClO_4^-. In other words, the sensitivity of the Hofmeister series electrode to anions other than perchlorate is insufficient to account for the magnitude of the sensor response. To definitively confirm the ClO_4^- detection, laboratory analyses using flight-spare and/or identical sensors were used to eliminate all other possibilities. The concentration of ClO_4^- in the Rosy Red, Sorceress-1 and Sorceress-2 soil samples have been reported ranging from 0.5 to 0.7 wt%; however recent reanalysis and refinements with decreased error (Fang *et al.* 2015) give solution concentrations of of 2.7, 2.2 and 2.5 mM, equivalent to 0.67, 0.68 and 0.62 wt% ClO_4^- in the soil, respectively (Table 1).

In addition to measuring the concentration of the ClO_4^- ion, the parent salt identity was determined by using the effect of the ClO_4^- ion on the calcium (Ca^{2+}) sensor. A series of laboratory analyses at various ratios of added $Mg(ClO_4)_2$ to $Ca(ClO_4)_2$ demonstrated that the response of the Ca^{2+} sensor would give the best fit to the WCL Mars data with a sample containing 60% $Ca(ClO_4)_2$ and 40% $Mg(ClO_4)_2$ (Kounaves *et al.* 2014a). The presence of $Ca(ClO_4)_2$ suggests that the soil at the Phoenix landing site has not been in contact with liquid water since formation. Subsequent dissolution of Ca $(ClO_4)_2$ in the presence of the soluble sulphates would have caused Ca^{2+} to precipitate as insoluble $CaSO_4$ (Kounaves *et al.* 2014b) and the ClO_4^- to reprecipitate as $NaClO_4$, $KClO_4$ and/or $MgClO_4$ (e.g. Marion *et al.* 2010; Toner *et al.* 2014). However, spectral analysis (0.455–1 μm) of the Phoenix soils is consistent with the presence of subsurface hydrated Mg-perchlorate patches that were interpreted to have formed by translocating Mg-perchlorate brines from the surface by liquid water thin films at low temperature (e.g. 206–245 K) (Cull *et al.* 2010). Mg-perchlorate deliquescent kinetics, although, may not be fast enough for the short periods of in which Mg-perchlorate brines are thermodynamically stable (Kounaves *et al.* 2014b). Nevertheless, more work is required to understand the possibility of post-depositional perchlorate translocation from the surface to the subsurface.

Even though the concentration of perchlorate present made it impossible to detect any other oxychlorine species like chlorate directly in the martian soil samples (Kounaves *et al.* 2010; Hanley *et al.* 2012), chlorate may be present in the Phoenix samples. Three recent discoveries, the presence of chlorate in the Mars meteorite EETA79001 (Kounaves *et al.* 2014b), the acquisition of orbital IR (1–3.92 μm) spectra consistent with the presence of hydrated Mg-chlorate (Ojha *et al.* 2015) and the formation of both ClO_4^- and ClO_3^- by UV on martian analogue Cl-bearing mineral surfaces (Carrier & Kounaves, 2015), strongly support this possibility. The detection of chlorate in EETA79001 actually occurred at a molar concentration 2.8 × higher than perchlorate (Kounaves *et al.* 2014b). Furthermore, chlorates commonly occur with perchlorates in terrestrial deserts, which suggest that if oxychlorine formation processes on Earth and Mars are similar then chlorates may occur wherever there are perchlorates on Mars (Rao *et al.* 2010).

Phoenix Scout Lander Thermal Evolved Gas Analyzer (TEGA)

The goal of the TEGA instrument was to search for organics and evaluate the volatile bearing mineralogy in surface sediments at the Phoenix Landing site. The TEGA instrument was composed of a scanning calorimeter coupled to a magnetic mass spectrometer (Hoffman *et al.* 2008; Boynton *et al.* 2009). Soils or sediments were scooped and deposited (~50 mg) into one of eight TEGA ovens. Soils were then heated to 1000°C at a heating rate of 20°C min^{-1} in a 12 mbar N_2 purge at 0.04 sccm flow rate (Boynton *et al.* 2009). Endothermic and/or exothermic transitions were detected by the scanning calorimeter and any volatile release or consumption was monitored simultaneously by the mass spectrometer. For example, evidence for the thermal decomposition of calcium bearing carbonate was

https://doi.org/10.1017/S1473550416000057

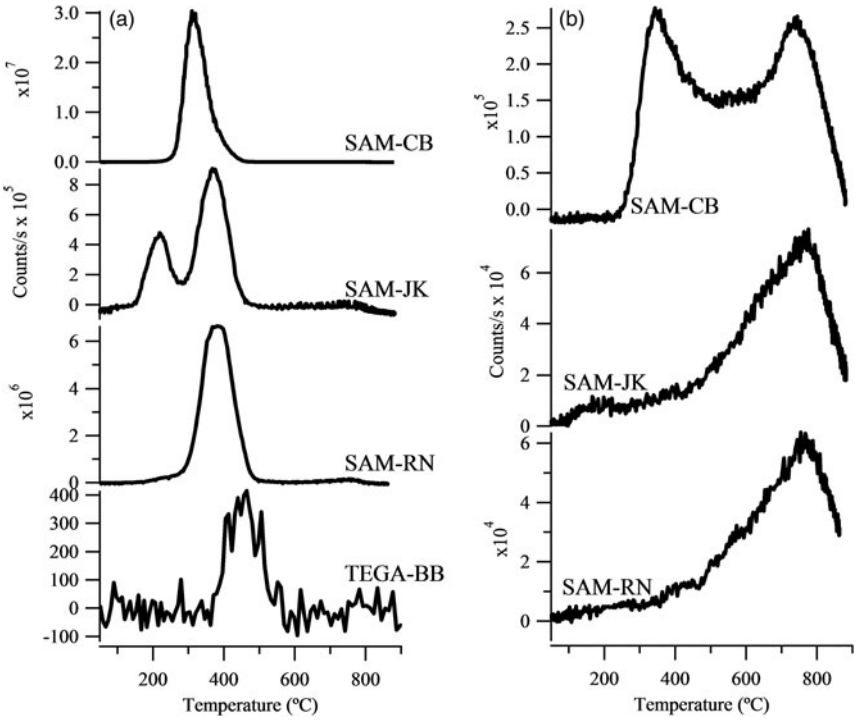

Fig. 2. (a) Evolved oxygen release versus temperature from the Phoenix Lander TEGA analysis of the Baby Bear (TEGA-BB) sample and the SAM–EGA of Gale Crater Rocknest (SAM-RN), John Klein (SAM-JK) and Cumberland (SAM-CB) samples. (b) Evolved HCl from the SAM–EGA of the SAM-RN, SAM-JK and SAM-CB materials. No Cl phases were detected by TEGA.

detected by presence of an endothermic transition and corresponding CO_2 detection (Boynton *et al.* 2009).

The detection of evolved O_2 by TEGA that began at 325°C and peaked at 465°C (Hecht *et al.* 2009) (Fig. 2(a)) is consistent with the presence of perchlorate in the Phoenix Landing site soil. Other O_2 sources are possible, but the detection of perchlorate by the WCL instrument indicates that perchlorate is the likely O_2 source. Perchlorate dehydration typically precedes its thermal decomposition (e.g. Marvin & Woolaver, 1945; Markowitz, 1963; Migdal-Mikuli & Hetmańczyk, 2008; Cannon *et al.* 2012).

Following dehydration, Na-, K- and Ca-perchlorate thermal decomposition results in O_2 evolution and chloride formation:

$$M^{z+}(ClO_4)_z \bullet nH_2O \grave{a} M^{z+}(ClO_4)_z + nH_2O \quad (1)$$

$$M^{z+}(ClO_4)_z \grave{a} MCl_z + z \bullet 2O_2 \quad (2)$$

Mg and Fe perchlorates dehydrate as above but instead form oxides and release Cl_2 gas.

$$2M(ClO_4)_2 \rightarrow 2MO + 7O_2 + 2Cl_2 \quad (3)$$

Any residual water vapour remaining in the oven area can react with the Cl_2 to from HCl

$$2Cl_2 + 2H_2O \rightarrow 4HCl + O_2 \quad (4)$$

Hydrated forms of perchlorate are thought to be stable under martian atmospheric conditions (e.g. Robertson & Bish, 2011) and evolved water detected by TEGA suggests that the perchlorate could have been hydrated, though adsorbed water and other hydrated minerals could have contributed to water detected by TEGA (Smith *et al.* 2009).

Perchlorate thermal decomposition is characterized by an exothermic transition (e.g. Acheson & Jacobs, 1970), yet no exothermic transition was observed by TEGA. The Phoenix soil possesses oxidized Fe phases that likely consist of nanophase iron oxides (Seelos *et al.* 2008; Goetz *et al.* 2010) which may have interacted with perchlorate and minimize the detection of the exothermic transition. Laboratory thermal analysis of K-perchlorate mixtures with hematite (Fe_2O_3) demonstrated that as more hematite was added, the intensity of the perchlorate decomposition exotherm decreased (e.g. Lee & Hsu, 2001). This suggests that interactions with Fe-oxide phases in the Phoenix material may have suppressed the perchlorate decomposition exotherm.

No evolved Cl masses (e.g. *m/z* 35 Cl, *m/z* 36 HCl, *m/z* 70 Cl_2) were detected by TEGA suggesting that either the perchlorate was Na, Ca or K-perchlorate or that Cl was removed from the gas stream by Ni-bearing components of the TEGA (Lauer *et al.* 2009). The Na-, K- and Ca-perchlorates mostly decompose to chloride phases with limited evolution of Cl (e.g. Marvin & Woolaver, 1945; Markowitz, 1963) indicating that perhaps these perchlorates are responsible for the O_2 release. However, laboratory analogue studies of the WCL ion selective electrode analyses were consistent with the presence of Mg-perchlorate and Ca-perchlorate (Kounaves *et al.* 2014a). This suggests that at least some HCl from Mg-perchlorate decomposition could have been detected. The possibility exists that the Ni composition of the TEGA ovens could have reacted

https://doi.org/10.1017/S1473550416000057

with evolved Cl species to form $NiCl_2$ and scrubbed the Cl from the gas stream and inhibit detection by the TEGA mass spectrometer (Lauer *et al*. 2009).

MSL-SAM instrument

Background

The main objectives of the SAM instrument were to search for evidence of organics and evaluate the volatile bearing mineralogy in the Gale Crater sediments (Mahaffy *et al*. 2012; Glavin *et al*. 2013; Leshin *et al*. 2013; Archer *et al*. 2014; McAdam *et al*. 2014; Ming *et al*. 2014; Freissinet *et al*. 2015). The SAM instrument is composed of two ovens connected to a quadrupole mass spectrometer (QMS), gas chromatograph (GC) and tunable laser spectrometerTLS. Soil, sediment or drilled material is acquired and deposited into sample cups (~45–135 mg) that is then transferred to one of two ovens. The material in the cup is heated to ~860°C at 35°C min^{-1} in a 0.8 sccm He purge held at 25 mbar. Direct analysis of the volatiles released from the sample over the entire temperature range is achieved in an evolved gas analysis (EGA) mode where a fraction (~1 : 800 split) of the gas flow was analysed directly by electron impact ionization and QMS. A select temperature range of gas is sent to the GCMS for organic analysis (Glavin *et al*. 2013; Ming *et al*. 2014; Freissinet *et al*. 2015). The gas is concentrated on a hydrocarbon trap cooled to 5°C and subsequently desorbed by heating to ~300°C followed by GC separation (GC-5: MXT-CLP, Siltek-treated stainless steel metal-chlorinated pesticides column, 30 m length, 0.25 mm internal diameter and 0.25 μm film thickness) before detection by the thermal conductivity detector (TCD) and the QMS (GCMS mode). The detailed description of the SAM-EGA and GCMS modes and instrument parameters can be found elsewhere (Mahaffy *et al*. 2012; Glavin *et al*. 2013).

SAM-EGA results

The SAM-EGA has detected O_2 and HCl releases in all samples reported to date suggesting the presence of perchlorate or chlorate in the Gale materials (Leshin *et al*. 2013; Glavin *et al*. 2013; Ming *et al*. 2014) (Fig. 2(a) and (b)). The Rocknest (RN) eolian deposit and John Klein (JK) and Cumberland (CB) mudstones all evolved O_2 and HCl during pyrolysis. However, laboratory analyses of pure perchlorate phases do not yield O_2 and HCl at temperatures entirely consistent with the Gale detections (Glavin *et al*. 2013; Leshin *et al*. 2013; Ming *et al*. 2014). Iron-bearing phases (e.g. hematite) when mixed with perchlorate or chlorate are known to lower perchlorate and chlorate decomposition temperatures (Rudloff & Freeman, 1970; Lee & Hsu, 2001). Iron-oxide phases detected by CheMin in the Gale sediments (Bish *et al*. 2013; Blake *et al*. 2013; Vaniman *et al*. 2014) suggest that such phases could lower the O_2 releases temperatures.

The amounts of O_2 for RN, JK and CB translates to 0.1–1.1 wt% ClO_4 or 0.1–1.2 wt% ClO_3 (Archer *et al*. 2014; Ming *et al*. 2014) (Table 1). The amount of HCl evolved (0.006–0.04 wt%) is much less than what is calculated to be

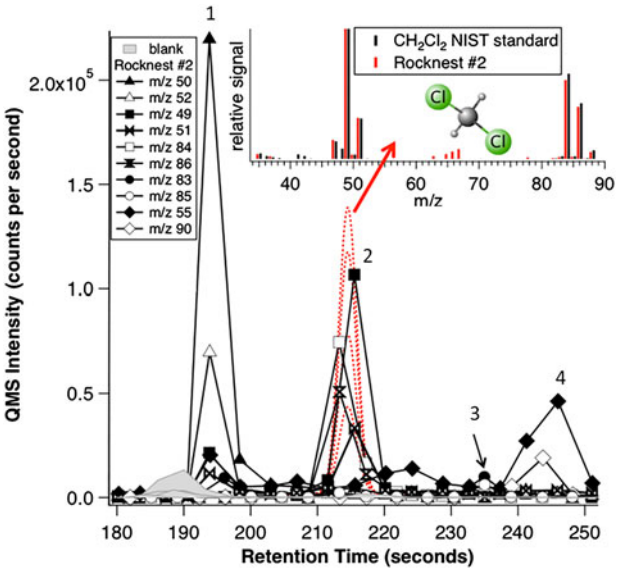

Fig. 3. SAM gas chromatogram showing the intensities (in counts per second) of the major masses of the chloromethanes and a chloromethylpropene detected in the second Rocknest sample run compared with the empty cup blank (shaded peaks) as a function of retention time in seconds. Each peak was identified by matching the mass spectrum generated from Gaussian fits of the QMS *m/z* values to mass spectra available in the NIST library (e.g. shown in inset). Peak identifications: 1, chloromethane; 2, dichloromethane; 3, trichloromethane; and 4, 1- or 3-chloro2-methylpropene. Figure from Glavin *et al.* (2013).

stochiometrically possible from O_2 releases, for chlorate or perchlorate. This suggests the presence of perchlorate/chlorate phases that do not evolve HCl may be present. For example, pure magnesium and iron perchlorate evolve HCl upon thermal decomposition, whereas Ca, Na and K-perchlorate do not evolve HCl (Markowitz, 1963). The presence of natural geologic materials, on the other hand, may promote complex reactions with the perchlorate/chlorate phases. Such complex reactions could alter the evolution of Cl and/or formation of chloride phases which may cause HCl release characteristics to differ from what is expected of pure perchlorate phases.

SAM–GCMS results

The SAM/GCMS along with SAM-EGA detected chlorinated hydrocarbons produced during pyrolysis of the Rocknest fines that suggests the presence of oxychlorine compounds in the deposit (Fig. 3). Similar results were obtained after analysis of the drilled samples at Yellowknife Bay (John Klein and Cumberland) and Pahrump Hills (Confidence Hills) and those results are described in detail by Ming *et al*. (2014) and Freissinet *et al*. (2015).

The source of the chlorinated hydrocarbons was attributed to a reaction between martian oxychlorine and terrestrial organic contamination. Several chlorinated hydrocarbons including chloromethane (CH_3Cl), dichloromethane (CH_2Cl_2), trichloromethane ($CHCl_3$), a chloromethylpropene (C_4H_7Cl) and chlorobenzene (C_6H_5Cl) were identified by GCMS

https://doi.org/10.1017/S1473550416000057

above background levels with chloromethane abundances up to 2.3 nmol (~2.3 parts-per-million assuming 50 mg sample) after pyrolysis of the Rocknest samples, but were not detected in the empty cup blank run analysed prior to the analysis of the Rocknest fines (Fig 3). Several products of N-methyl-N-(tert-butyldimethylsilyl)-trifuoroacetamide (MTBSTFA), a chemical whose vapours were released from one of the derivatization cups inside SAM, were also identified in both the blank and Rocknest EGA and GCMS runs (Glavin *et al*. 2013). The evolution of the chloromethanes observed directly by EGA during pyrolysis was coincident with the increase in both O_2 and HCl released from the Rocknest sample at temperatures above ~200°C and the decomposition of one of the hydrolysis products of MTBSTFA, 1,3-bis(1,1-dimethylethyl)-1,1,3,3-tetramethyldisiloxane. These correlations strongly suggest that the chlorinated hydrocarbons detected by SAM are the result of reactions between MTBSTFA products and O_2 and Cl released from the decomposition of an oxychlorine species during pyrolysis.

Laboratory pyrolysis GCMS analyses of 1 wt% Ca- and Mg-perchlorate mixtures heated in the presence of μmol quantities of MTBSTFA consistently showed the same distribution of chloromethanes and chloromethylpropene that were detected by SAM–GCMS. Although Cl_2 is predicted to form from the decomposition of Mg-perchlorate, Cl_2 was not detected in the SAM–GCMS data. Any Cl_2 that was released from perchlorates was likely converted to HCl during pyrolysis or on the hydrocarbon trap due to the much higher quantities of H_2O released from the sample (e.g. reaction 4). The presence of oxychlorine species in Rocknest are thus indicated by the chlorinated hydrocarbons detected by SAM which are likely products of reactions between martian oxychlorine species and terrestrial organic carbon in SAM (e.g. MTBSTFA and associated products) and martian oxychlorine species in the samples (Glavin *et al*. 2013). Subsequent work, however, has identified martian organics including chlorobenzene and a C_2, C_3 and C_4 dichloroalkane that could only be due to reactions between martian organics and oxychlorine in the Cumberland mudstone (Freissinet *et al*. 2015).

The abundances of chloromethane and dichloromethane measured by the SAM/GCMS at Rocknest (up to ~2 ppm) were much higher than the trace amounts of these simple chlorinated hydrocarbons (0.04–40 ppb) detected by the Viking 1 and Viking 2 lander GCMS instruments (Biemann *et al*. 1976, 1977). The chloromethane and dichloromethane detected in the Viking near surface soil runs were originally thought by Biemann *et al*. (1977) to be derived from terrestrial sources including cleaning solvents. However, similar to SAM, these chloromethanes were not identified in empty oven blank GCMS runs carried out by both Viking landers prior to the analysis of the soils. Although perchlorates were not identified at the Viking landing sites, the detection of perchlorate at the Phoenix (Hecht *et al*. 2009) Gale Crater landing sites (Glavin *et al*. 2013; Ming *et al*. 2014) suggests that both Viking Lander GCMS instruments measured signatures of perchlorates or other oxychlorine compounds (Navarro-González *et al*. 2010) in the form of chloromethane and dichloromethane. This will be further discussed below. The much higher abundances of chloromethanes detected in the Rocknest soil by SAM compared with the abundances measured at the Viking sites is likely due to a significant terrestrial carbon background from MTBSTFA in SAM that was not present in the Viking GCMS instruments.

The possibility that phases other than oxychlorine phases may be responsible for the detected O_2 are possible but unlikely. Nanomole levels of nitrogen-oxide (NO, *m/z* 30) were detected and were attributed to nitrate thermal decomposition at similar temperatures as the main O_2 releases (Leshin *et al*. 2013; Ming *et al*. 2014; Stern *et al*. 2015). Nitrate thermal decomposition results in O_2 evolution, but the nmole levels of nitrates would not be expected to contribute significantly to the μmole O_2 detections. The detected high temperature (>500°C) SO_2 releases are consistent with sulphate thermal decomposition (Ming *et al*. 2014; McAdam *et al*. 2014) that can also evolve O_2. However, sulphate thermal decomposition occurring above 500°C is not a likely candidate for the main O_2 releases detected below 500°C. Hydrogen peroxide has been proposed to be a potential oxidant in the martian soil, but thermal decomposition of hydrogen peroxide occurs below 145°C and thus is not a candidate O_2 source in the Gale Crater sediments (Zent & McKay, 1994; Wu *et al*. 2010). Superoxides are another proposed source of O_2 but their instability in the presence of water (e.g. Yen *et al*. 2006) suggests that any O_2 related superoxides would have evolved with the main H_2O releases that occur below 200°C. The SAM-EGA and GCMS detections of O_2, HCl and a variety of chlorinated hydrocarbons produced during pyrolysis of the Rocknest scooped aeolian fines and in multiple drilled mudstone samples collected by Curiosity strongly argue for the presence of martian oxychlorine compounds such as perchlorates and/or chlorates.

Viking GCMS

The overall goal of the Viking GCMS analyses was to search for organics in the martian surface material. The detection of chlorinated hydrocarbons at the Viking Landing sites was thought to be derived solely from terrestrial contamination (Biemann *et al*. 1976, 1977). The detection of perchlorate at the Phoenix Landing site promoted a revaluation of the Viking GCMS analysis, which suggested chlorinated hydrocarbon Cl could be derived from martian oxychlorine (e.g. ≤0.1 wt% perchlorate) in the Viking regolith (Navarro-González *et al.* 2010). Two regolith samples at each of the Viking Landing sites, Chryse Planitia (VL-1) and Utopia Planitia (VL-2), were analysed using thermal volatilization coupled to GCMS. The first VL-1 sample was acquired on Sol 8 and was primarily comprised of fine-grained material collected from 4 to 6 cm below the surface. A single ~100 mg fraction of this sample was delivered to GCMS oven number 1 analysed on sols 17 and 23 (Biemann *et al*. 1976). The second VL-1 sample was collected on sol 31 and consisted of coarse surface material located ~3 m from the sol 8 sample collection site. A single ~100 mg fraction of this sample was delivered to VL-1 oven 2 and analysed and on sols 32, 37 and 43. The first

https://doi.org/10.1017/S1473550416000057

Table 2. *Viking 1 and 2 GCMS results for methyl chloride (CH_3Cl) (scan 27) and methylene chloride (CH_2Cl_2) (scan 89)*

						CH_3Cl		CH_2Cl_2	
Mission	Oven	Sample	Sol analysed	Purge gas	Temp.°C	Split	ppb	Split	ppb
VL1	1	Blank	Cruse	$^{13}CO_2$	500	–	ND	0 : 1	ND
	1	Subsurface	17	$^{13}CO_2$	200	3 : 1	15	20 : 1	ND
	1	Subsurface	23	$^{13}CO_2$	500	>20 : 1	ND	20 : 1	ND
VL1	2	Surface	32	$^{13}CO_2$	350	Closed	ND	20 : 1	ND
	2	Surface	37	$^{13}CO_2$	500	Closed	ND	20 : 1	ND
	2	Surface	43	$^{13}CO_2$	500	Closed	ND	20 : 1	ND
VL2	2	Blank	Cruse	$^{13}CO_2$	500	0 : 1	ND	0 : 1	ND
	2	Duricrust	24	H_2	200	20 : 1	ND	0 : 1	ND
	2	Duricrust	26	H_2	350	400 : 1	ND	0 : 1	6–14
	2	Duricrust	35	H_2	500	400 : 1	ND	0 : 1	6–14
	2	Duricrust	37	$^{13}CO_2$	500	3 : 1	ND	0 : 1	2–6
VL2	3	Under Rock	41	H_2	50	0 : 1	ND	0 : 1	ND
	3	Under Rock	43	H_2	200	400 : 1	ND	0 : 1	0.04–0.08
	3	Under Rock	45	H_2	350	400 : 1	ND	0 : 1	10–20
	3	Under Rock	47	H_2	500	400 : 1	ND	20 : 1	<4
	3	Under Rock	61	$^{13}CO_2$	500	Blocked	ND	0 : 1	20–40

(Biemann *et al.* 1976, 1977).

VL-2 GCMS sample, a surface duracrust, was collected on sol 21 and a single ~100 mg fraction was analysed four times (sols 24, 26, 35 and 37) using VL-2 oven 2. The second VL-2 sample was acquired on sol 37 from under Badger Rock and a single ~100 mg fraction was analysed five times (sols 41, 43, 45, 47 and 61) using VL-2 oven 3 (Biemann *et al.* 1977) (Table 2).

The Viking GCMS instruments and sample analysis protocols (Biemann *et al.* 1974; Rushneck *et al.* 1978) differed substantially from both the Phoenix TEGA (Boynton *et al.* 2009) and MSL-SAM (Mahaffy *et al.* 2012) instruments, and consequently the results differed considerably. The TEGA and SAM instruments employed temperature ramps to perform sample thermal volatilization, in contrast, the Viking GCMS instruments, used temperature steps (50, 200, 350 and 500°C) with a 30 s hold time. Also the TEGA and SAM instruments utilized N_2 and He carrier gases, respectively, in a flow-through thermal volatilization mode while the Viking GCMS sample thermal volatilization was performed in a sealed sample cell (i.e. no flow) with either a H_2 or $^{13}CO_2$ filled headspace. After the volatilization step, carrier gas (H_2) was diverted through the sample cell to inject the sample gases into the Viking GC column. Two other significant differences between the TEGA and SAM instruments and the Viking GCMS, both of which were used to protect the Viking MS from high pressure, were the use of a heated Ag–Pd diffusion tube to reduce the H_2 purge gas pressure prior to the MS entrance and the use of a pressure sensitive effluent divider which acted to split and divert fractions of the carrier gas away from the MS as needed. For example as shown in Table 1, 20 : 1 ratio indicates that 20 parts were vented and one part of the gas from the GC column was sent to the MS.

The use of H_2 carrier gas in combination with the heated Ag–Pd diffusion tube prevented the detection of O_2 (g) due to its reduction into H_2O (g) prior to entry into the MS. This limitation, along with the lack of a direct EGA mode (i.e. direct MS injection), eliminates the ability to use O_2 (g) release from the sample as a diagnostic for the presence of perchlorate or other oxychlorine species as was done with the TEGA (Boynton *et al.* 2009) and SAM data sets (Leshin *et al.* 2013; Glavin *et al.* 2013; Ming *et al.* 2014). These factors leave the detection of trace amounts of chloromethane (CH_3Cl) in the VL-1 subsurface sample and trace amounts of dichloromethane (CH_2Cl_2) in both VL-2 samples as the sole GCMS evidence for the presence of volatile chlorine species in the Viking samples.

At the time of the initial Viking GCMS analyses, the possibility that the detected CH_3Cl and CH_2Cl_2 might be of martian origin was recognized, however, the detection was attributed potential instrument contamination (Biemann *et al.* 1979). After the discovery of perchlorate during the Phoenix mission, the suggestion was made that the Viking GCMS CH_3Cl and CH_2Cl_2 detection was due to the presence of perchlorate and organics indigenous to the samples (Navarro-González *et al.* 2010); an interpretation that was subsequently debated in the literature (Biemann & Bada, 2011; Navarro-González & McKay, 2011).

Chloromethane was detected during VL-1 sample analyses and dichloromethane was detected during VL-2 analyses (Table 2). The VL-1 subsurface sample analysis detected 15 ppb of CH_3Cl during the first sample heating (200°C) on sol 17. No CH_3Cl was detected during the second sample heating (500°C) on sol 23, and no CH_2Cl_2 was detected in either run. The position of the effluent divider at different times during the sample runs may offer a possible explanation as to why for CH_3Cl was only detected in the first VL-1 sample run. During the first run of the *subsurface* sample, the effluent divider was in a 3 : 1 split at scan number 27 (which corresponds to the elution time of CH_3Cl). In contrast, the effluent divider was in a 20 : 1 split ratio, indicating less gas from the GC column was sent to the MS detector, during scan 89 (corresponding to the elution time of CH_2Cl_2), which may have precluded the detection of CH_2Cl_2. Likewise, in the analyses of the

https://doi.org/10.1017/S1473550416000057

VL-1 *surface* sample the effluent divider was closed (carrier gas fully vented) during scan 27 and in a 20 : 1 split ratio during scan 89. These divider positions may have prevented the detection of low levels of CH_3Cl and CH_2Cl_2, generated from VL-1 samples, except when effluent divider was in the lower 3 : 1 split (i.e. during the first run of the subsurface sample at scan 27). Although an in-cruise blank run using the VL-1 oven 1 was performed no CH_4 or CH_3Cl was detected in this run. Despite a 0 : 1 split ratio at scan 87, no CH_2Cl_2 (Table 2) or other hydrocarbons were detected in the VL-1 blank run except for trace amounts of Freon-E (Viking cleaning solvent) (Biemann *et al.* 1976, 1977), which is an unlikely precursor to CH_3Cl.

Dichloromethane was detected in almost all VL-2 duracrust and Badger Rock sample runs; however, CH_3Cl was not detected in any of the VL-2 runs. As was the case for the lack of CH_2Cl_2 detection in the VL-1 data, the lack of CH_3Cl detection may possibly be explained by the position of effluent divider during the time of CH_3Cl elution. At scan 89, which corresponds to the elution time of CH_2Cl_2 the effluent divider was in a 0 : 1 split ratio, that is all of the carrier gas was directed into the GC column for all runs except the fourth Badger rock run in which case the divider was in a 20 : 1 ratio position. While for most VL-2 runs the effluent divider was in a 400 : 1 split during scan 27, when CH_3Cl would be expected to elute, thus making it difficult to detect CH_3Cl.

The apparent incomplete decomposition of perchlorate as indicated by the repeated detection of CH_2Cl_2 from each of the two VL-2 samples suggests that the proposed concentrations of perchlorate inferred from the Viking GCMS results should be considered a minimum. Because each Viking sample was analysed multiple times, the total amount of CH_2Cl_2 detected from the VL-2 duracrust sample was 14–32 ppb and the total amount detected from the VL-2 Badger Rock sample was ~34–64 ppb. Furthermore, the detectable levels of CH_2Cl_2 detected in the final run for each VL-2 sample indicates that not all of the volatile chlorine was released (i.e. the CH_2Cl_2 did not go to zero). Likewise, the 15 ppb of CH_3Cl detected in the VL-1 subsurface run should be considered a minimum because only two runs were performed. The partial decomposition of perchlorate is consistent with the SAM and TEGA results that show relatively slow perchlorate decomposition kinetics occurring over an extended heating period as indicated by O_2 and Cl (measured as HCl) evolution over a wide temperature range from the Gale samples sample (Fig. 2).

The possibility that the organic sources of the chlorinated hydrocarbons detected with the Viking GCMS instrument were of martian origin has been questioned (Biemann & Bada, 2011; Navarro-González & McKay, 2011). The organic sources for the chlorinated hydrocarbons detected by SAM–GCMS have been attributed to terrestrial and martian sources (Glavin *et al.* 2013; Freissinet *et al.* 2015). Chlorobenzene was not detected by the Viking-GCMS but was detected by SAM analyses. The SAM chlorobenzene detection was attributed to the reaction of martian perchlorate thermal decomposition products with both hydrocarbon contamination generated by Tenax sample preconcentrators in the GC system, and to indigenous martian organics (Glavin *et al.* 2013; Ming *et al.* 2014; Freissinet *et al.* 2015). Although benzene contamination may be a poor chlorobezene precursor (Freissinet *et al.* 2015), the Viking data provides no evidence for the presence of indigenous aromatic organics that may serve as a chlorobenzene precursor (e.g. aromatic carboxylic acids). Additionally, dichloroalkanes were not detected in the Viking GCMS runs, however, they were detected in the SAM runs and, as was the case for the SAM chlorobezene detections, attributed to both terrestrial organic contaminates and indigenous martian organics (Freissinet *et al.* 2015). Similarly, trichloromethane sourced from martian perchlorate-Cl reacting with terrestrial background hydrocarbons was detected by the SAM–GCMS but not detected by Viking-GCMS. Independent of the origin of the hydrocarbon component (contamination or indigenous to Mars) of the detected CH_3Cl and CH_2Cl_2, the lack of the detection of chlorine in the Viking GCMS blank runs, as with the MSL-SAM data (Glavin *et al.* 2013) strongly suggests a martian origin for the chlorine that is consistent with presence of perchlorate and possibly other oxychlorine species.

Mars science laboratory Chemistry and Mineralogy (CheMin) instrument

The CheMin instrument on MSL performs XRD and X-ray fluorescence (XRF) on scooped soil and drilled rock samples (Blake *et al.* 2012, 2013; Bish *et al.* 2013; Vaniman *et al.* 2014). Samples are sieved to <150 μm before delivery into a disc-shaped sample cell 8 mm in diameter and 175 μm thick. CheMin uses a Co X-ray source and operates in transmission geometry. A collimated X-ray beam strikes the sample cell, while the sample is agitated by piezoelectric vibrations to achieve different orientations of the grains. Diffracted X-ray photons are detected by a cooled charge coupled device in a two-dimensional (2D) array. The 2D ring patterns are integrated circumferentially to obtain conventional 1D diffraction patterns. CheMin's angular range is ~5–50°2θ with 0.3°2θ full-width at half-maximum resolution at 25°2θ. These large instrumental peak widths (relative to laboratory X-ray diffractometers) limit the ability to accurately determine minor crystalline phases, so that the detection limit of CheMin is ~1–3 wt%. Abundances of crystalline phases and crystal structures of these phases are determined by the Rietveld refinement method (e.g. Young, 1993), whereas abundances of amorphous, poorly crystalline, and phyllosilicate phases (i.e. poorly ordered phases) are determined by the FULLPAT full-pattern fitting method (Chipera & Bish, 2002).

SAM data suggest that the abundances of oxychlorine compounds in the Gale Crater sediments are near the detection limit of CheMin (Leshin *et al.* 2013; Ming *et al.* 2014); however, Rietveld refinements of CheMin data from the Rocknest, John Klein and Cumberland samples have not unequivocally identified oxychlorine minerals (Bish *et al.* 2013; Vaniman *et al.* 2014). Akaganeite, β-$Fe^{3+}O(OH,Cl)$, has been detected in CheMin data of John Klein and Cumberland, but for this discussion, akaganeite will not be included as an oxychlorine phase.

https://doi.org/10.1017/S1473550416000057

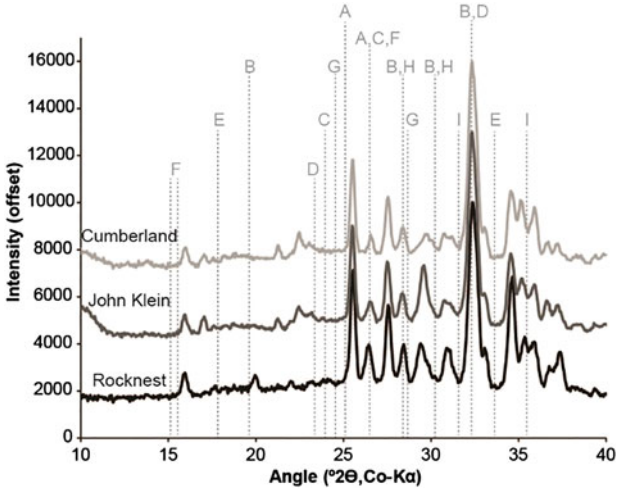

Fig. 4. Chemistry and Mineralogy (CheMin) instrument data for the Rocknest, John Klein and Cumberland samples (patterns are offset vertically for clarity, and data >40°2θ are excluded to focus on the region where oxychlorine minerals have reflections. Dashed vertical lines denote the positions of strong XRD peaks of Fe (II)-perchlorate•6H_2O (A), Fe(III)-perchlorate•9H_2O (B), Ca-perchlorate•6H_2O (C), anhydrous Ca-chlorate (D), Ca-chlorate•2H_2O (E), Mg-chlorate•6H_2O (F), anhydrous Na-perchlorate (G), Na-perchlorate•1H_2O (H) and anhydrous Na-chlorate (I). Note: Dashed lines are for indication purposes and do not imply relative intensities of peaks.

Comparisons of laboratory EGA data to SAM data from Rocknest, John Klein, and Cumberland suggest that Ca, Mg and/or Fe perchlorates are possible oxychlorine compounds that contribute to the O_2 and HCl signals (Leshin *et al.* 2013; Glavin *et al.* 2013; Ming *et al.* 2014). Perchlorate minerals can have several hydration states, dependent on relative humidity (RH) and temperature conditions. A range of perchlorate hydration states for Mg-perchlorate, for example, were evaluated at temperatures and RH relevant to Mars and it was determined that $Mg(ClO_4)_2$•6H_2O would be the most stable phase on the martian surface (Robertson & Bish, 2011). Hydrated Mg-perchlorate [$Mg(ClO_4)_2$•6H_2O] and Ca-perchlorate [$Ca(ClO_4)_2$•4H_2O] were included in Rietveld refinements of CheMin data of Rocknest (Bish *et al.* 2013) and John Klein and Cumberland (Bish, personal communication); however, these phases refined to zero indicating that these hydrated perchlorates are not present.

Visual comparisons of the XRD patterns of additional perchlorate and chlorate phases available in the International Centre of Diffraction Data (ICDD) library to the CheMin XRD patterns from Rocknest, John Klein, and Cumberland do not support the presence of crystalline perchlorate or chlorate minerals (Fig. 4). Considering the low abundance of oxychlorine phases in samples from Gale crater and the high background in CheMin data from a significant amorphous component, only the strongest XRD lines of oxychlorine minerals would be detectable in CheMin data. The strongest peaks of some oxychlorine minerals, including Fe(II)-perchlorate•6H_2O, anhydrous Ca-chlorate, anhydrous Na-perchlorate, Na-perchlorate•H_2O and anhydrous Na-chlorate overlap peaks of common basaltic igneous minerals, so that it would be difficult to detect them in many soils and sediments on Mars (Fig. 4). Strong peaks of other oxychlorine minerals occur at angles lower than common basaltic minerals, so that they could be more easily detected, including Fe(III)-perchlorate•9H_2O, Ca-perchlorate•6H_2O, Ca-chlorate•2H_2O and Mg-chlorate•6H_2O. Investigations of these regions of CheMin XRD patterns from Rocknest, John Klein and Cumberland show no evidence for these phases (Fig. 4).

Although oxychlorine minerals may be at the detection limit of CheMin, the detection limit is dependent upon the crystallinity of the phase in question and the positions of the strongest XRD lines of that phase. If the oxychlorine phase is poorly crystalline, so that its XRD peaks are broad, then its detection limit with CheMin is much greater than 1–3 wt% (e.g. Bish *et al.* 2013). The low ionic potential of perchlorate and chlorate ions in solution and the very low eutectic temperatures of both perchlorate and chlorate salts may help them precipitate from solution as amorphous phases in martian soils (Toner *et al.* 2014). If the oxychlorine phase in the Gale sediments is completely amorphous, then it would be undiscernible from other amorphous materials and would contribute to the amorphous hump (i.e. broad, convex-upward background) observed in all CheMin analyses to date (e.g. Rampe *et al.* 2014).

The possibility of a mixture of chlorate and perchlorate also presents a challenge to the CheMin detection of oxychlorine phases in the Gale sediments. The chlorate anion is the most stable intermediate species of the oxidation of chloride to perchlorate (e.g. Hanley *et al.* 2012), and concentrations of perchlorate and chlorate can be equivalent in desert soils on Earth (Rao *et al.* 2010). The subdivision of the oxychlorine concentrations as detected by SAM into equal portions of perchlorate and chlorate would easily cause the individual perchlorate and chlorate abundances to fall below the detection limits of CheMin.

IR spectroscopy

Perchlorates and chlorates have diagnostic spectral features throughout the visible/near-IR (VNIR; ~0.35–2.5 μm) and mid-IR (~5–50 μm). The VNIR features of perchlorates have been characterized using reflectance spectroscopy techniques similar to those used by VNIR spectrometers on remote sensing platforms in orbit around Mars (Morris *et al.* 2009; Cull *et al.* 2010; Bishop *et al.* 2014; Hanley *et al.* 2015). Mid-IR studies of perchlorates and chlorates (Miller & Wilkins, 1952; Pejov & Petruševski, 2002; Bishop *et al.* 2014; Hanley *et al.* 2015) have utilized reflectance and absorption spectroscopic techniques, which differ substantially from mid-IR emission spectroscopy technique employed at Mars. All of these studies demonstrate that oxychlorine salts have numerous diagnostic spectral features in the mid-IR. These studies show that the anion (ClO_4^- or ClO_3^-), cation (Na^+, Mg^{2+}, Ba^{2+}, Ca^{2+}, K^+, etc.) and hydration state all cause systematic variations in the mid-IR spectral properties, making mid-IR spectroscopy a useful diagnostic tool for oxychlorine

https://doi.org/10.1017/S1473550416000057

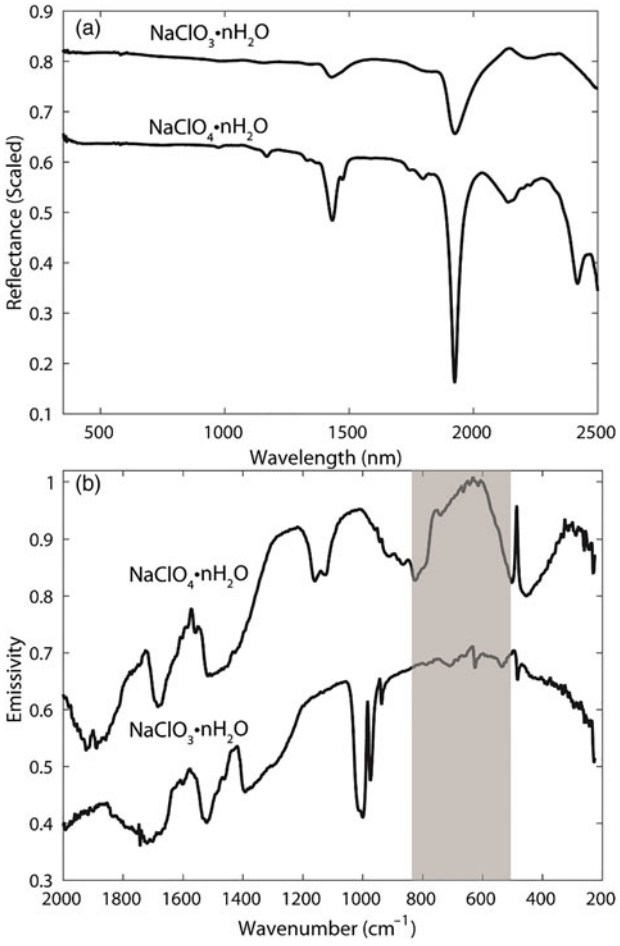

Fig. 5. (a) Reflectance and (b) thermal emissivity spectra of sodium chlorate and sodium perchlorate. Shaded region (507–825 cm^{-1}) in (b). indicates region obscured by atmospheric CO_2.

salts. However, the exact positions, shapes, and intensities of bands vary between measurement techniques (e.g. absorption, reflectance, emissivity). To directly compare laboratory spectra to remote sensing data sets, mid-IR emissivity measurements acquired under appropriate conditions are required. To date, such a database of chlorate and perchlorate salts is not available.

Previous studies have shown that the VNIR reflectance spectra of perchlorates are dominated by the modes of hydration of these samples, and that anhydrous perchlorates have no strong spectral features in the 0.35–2.5 μm spectral range (Morris *et al.* 2009; Cull *et al.* 2010; Bishop *et al.* 2014; Hanley *et al.* 2015; Ojha *et al.* 2015). Bidirectional reflectance spectra of hydrated Na chlorate and perchlorate (Sigma Aldrich reagent grade) were collected to illustrate the characteristic spectral features of hydrated Na chlorate and Na perchlorate. Example spectra were acquired on an ASD FieldSpec3 Max spectrometer at Stony Brook University's Vibrational Spectroscopy Laboratory (VSL) (Fig. 5(a)). Spectra were acquired under ambient conditions with 30° and 0° incidence and emergence angles, respectively, and referenced to an isotropic white spectralon target. A total of 100 spectra of each sample were averaged to create final spectra.

Hydrated Na perchlorate displays two strong bands at 1.43 and 1.93 μm, with additional weaker bands between 1.00 and 2.33 μm (Fig. 5(a)). Hydrated Na chlorate has a more complex spectrum, with major bands at 1.43 and 1.92 μm, with additional weaker bands at between 0.97 and 2.42 μm. The large number of bands may be due to several hydration states being present in the sample. Regardless, it is clear from these data and those of others (e.g. Morris *et al.* 2009; Cull *et al.* 2010; Bishop *et al.* 2014), that perchlorates are best identified in the VNIR wavelength region by the positions and shapes of their various H_2O vibrational bands. The major perchlorate/chlorate hydration bands at ~1.4 and 1.9 μm are noted as overlapping with other H_2O or OH bands from other hydrated phases including sulphates and phyllosilicates, which are also known to occur on Mars. Although the band shapes and exact positions may vary between oxychlorine species, the potential presence of other hydrated phases (e.g. sulphates, phyllosilicates) indicates that care must be taken when determining the presence or absence of oxychlorine from remotely sensed VNIR data.

Figure 5(b) shows mid-IR emissivity spectra of hydrated Na perchlorate and chlorate acquired on VSL's Nicolet 6700 FTIR spectrometer modified to collect emissivity spectra by removing the glowbar IR source and exposing the interferometer to a custom-built environmental chamber. Samples were heated to 80°C and spectra were collected in an environment with CO_2 and H_2O vapour removed. Spectra were referenced to a blackbody calibration target heated to 70° and 100°C and were calibrated using the methods of Ruff *et al.* (1997). A total of 256 spectra of each sample were averaged to create the final spectra.

The major features in the mid-IR emissivity data are due to ClO_4 bending and stretching modes. The positions and shapes of the Na perchlorate spectrum are generally similar to those reported in the reflectance data by Bishop *et al.* (2014). The hydrated Na chlorate spectrum has fewer strong features than perchlorate at long wavelengths (12.5–50 μm; 200–800 cm^{-1}), but has a strong split ClO_3 stretching mode at 1000 cm^{-1}. The multiple strong spectral features of chlorates and perchlorates in the mid-IR make them good candidates to be identified in thermal emission remote sensing data sets if their concentrations are high enough anywhere on the martian surface (≳5–10 vol%).

IR evidence consistent with presence of hydrated perchlorate and/or chlorate has been detected in select locations on Mars by orbital and landed IR analyses. The Phoenix Lander's Surface Stereo multispectral visible/IR (0.45–1.00 μm) imager has detected an IR hydration feature consistent with the presence of hydrated perchlorates in discrete, concentrated patches at the Phoenix landing site (Cull *et al.* 2010). The Mars Reconnaissance Orbiter's CRISM instrument has also detected hydration features in the VNIR range (6–18 m $pixel^{-1}$ spatial resolution) consistent with the presence of hydrated perchlorate and chlorate at several locations associated with martian RSL features (Ojha *et al.* 2015).

Anhydrous chloride salts have also been remotely detected from orbit using both mid-IR and VNIR instruments (Fig. 6). Chloride salt deposits were initially identified in mid-IR Thermal Emission Imaging System (THEMIS)

https://doi.org/10.1017/S1473550416000057

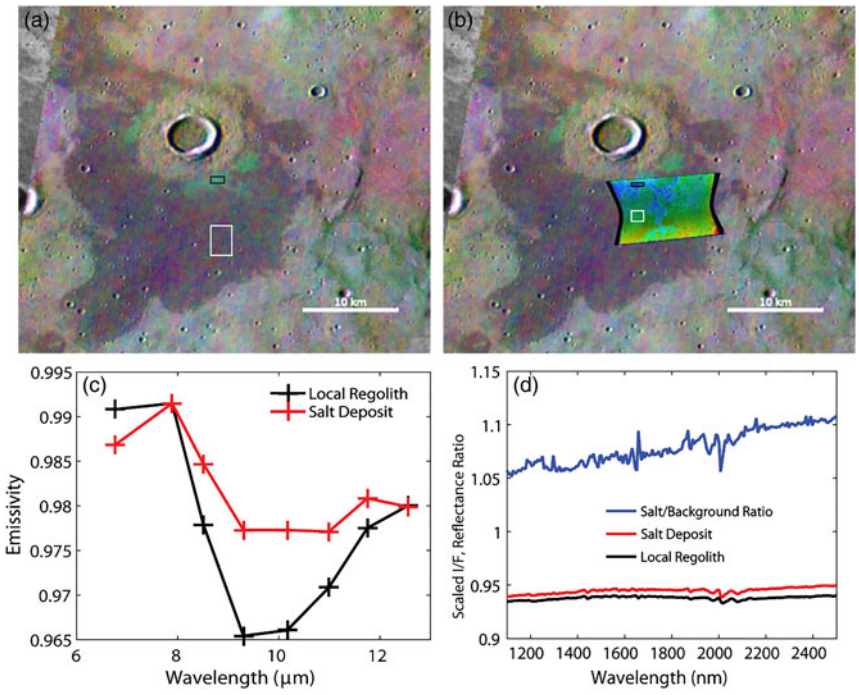

Fig. 6. Examples of THEMIS and CRISM data covering chloride-bearing deposits on Mars in Noachis Terra. Images are centered at 347.1E, −40.6N. (a) THEMIS decorrelation stretched image mosaic utilizing band 9, 6 and 4 as R, G and B. Chloride deposits appear bright green around the ejecta of the crater located in the center of the figure. The black (chloride) and white (background regolith) boxes show the locations for spectra displayed in Fig. 6(c) from THEMIS image I15341006. (b) The ISLOPE parameter from CRISM image FRT000109DF overlayed on the THEMIS mosaic. Bright blue areas (negative parameter values) are a good proxy for chloride deposits. The black (chloride) and white (background regolith) boxes show the locations for spectra displayed in Fig. 6(d). (c) THEMIS spectra acquired both on and off the chloride salt deposit. The chloride deposit exhibits shallower spectral contrast and a slight blue slope compared with the regional regolith. (d) CRISM ratio I/F spectrum of the chloride deposit, showing a generally featureless red slope. Features near 2000 nm are atmospheric artefacts. The chloride deposit and local regolith spectra used to make the ratio spectrum are also shown.

multispectral images ($\sim$100 m pixel^{-1} spatial resolution) (Osterloo *et al.* 2008). These detections were subsequently supported by observations made at VNIR wavelengths with the CRISM instrument (Murchie *et al.* 2009; Wray *et al.* 2009; Glotch *et al.* 2010) and the Observatoire pour la Minéralogie, l'Eau, les Glaces et l'Activité (OMEGA) instrument (Ruesch *et al.* 2012). Anhydrous chloride salts have no features at either VNIR or mid-IR wavelengths. At VNIR wavelengths, CRISM and OMEGA ratio spectra of chloride salt-bearing surfaces are spectrally featureless, with a distinct red slope (Fig. 6). This spectral behaviour was confirmed in the laboratory, using physical mixtures of halite and flood basalt particulates (Jensen & Glotch, 2011). At mid-IR wavelengths, chloride salts are spectrally featureless and have an emissivity less than unity. This leads to distinct blue spectral slopes observed in THEMIS and thermal emission spectrometer (TES) data (Osterloo *et al.* 2008, 2010; Glotch *et al.* 2010) and laboratory emissivity spectra (Glotch *et al.* 2013, 2016). Recently acquired mid-IR emissivity spectra of the Jensen & Glotch (2011) halite/basalt sample suite, in combination with a hybrid light scattering/Hapke radiative transfer model has constrained the salt abundance at Martian chloride deposits to $\sim$10–25 vol%, with the remaining component being the regional silicate regolith (Glotch *et al.* 2013, 2016).

Despite the orbital IR detections of hydrated-perchlorate and hydrated-chlorate in select martian RSL features, chlorate or perchlorate have not been identified in the chloride bearing regions by IR remote sensing instruments orbiting Mars (Glotch *et al.* 2010; Osterloo *et al.* 2008, 2010). This is in stark contrast to hyperarid deserts (e.g. Atacama Desert, Antarctic Dry Valleys), where halide salts and silicates are often mixed or layered with various other phases such as nitrates, perchlorate and chlorate phases (e.g. Sutter *et al.* 2007; Rao *et al.* 2010; Jackson *et al.* 2015). Furthermore, the detection of oxychlorine phases at the Phoenix and Gale Crater landing sites suggests that where Cl concentrations are high as in these martian chloride deposits, perchlorates/chlorates should be present, but have yet to be detected by orbital IR analyses. As will be discussed below, the oxychlorine/total Cl ratio has been shown to vary between and within landing sites. Thus it is likely that concentration of oxychlorine phases in these chloride bearing regions is below orbital IR detection limits.

Total Cl versus oxychlorine relationships

The detection of oxychlorine species at the Phoenix, Gale Crater, RSL features and arguably at the Viking landing sites suggests that oxychlorine formation on Mars is likely a

https://doi.org/10.1017/S1473550416000057

global process. Chlorine analysis of sediments at the Phoenix and Gale Crater landing sites suggests that global martian Cl should contain an oxychlorine-Cl component that can range from 10 to 86 mol% of total measured Cl. The average soluble perchlorate and chloride concentration in the three sample solutions analysed by WCL at the Phoenix landing site was 2.5 ± 0.1 and 0.4 ± 0.2 mM, respectively (Fang *et al.* 2015). The molar oxychlorine-Cl amount in the Phoenix soils could therefore be ∼86% of the total chlorine in the sample. Gale Crater total Cl as determined by the Alpha Proton X-ray Spectrometer (APXS) and oxychlorine as determined by SAM-EGA indicate that the oxychlorine-Cl molar fraction is lower relative to the Phoenix landing site and varies from ∼10 to 40% of total Cl (Archer *et al.* 2015). This suggests that if the molar Cl in oxychlorine is only 10% of the total Cl in a 25 vol% chloride bearing region, then the oxychlorine phases could occur below the THEMIS detection limits (∼5–10 vol %).

Oxychlorine and total Cl data from the Phoenix and Gale landing sites may be used to constrain oxychlorine levels at sites where only total Cl data is available. Total chlorine has been determined for a wide variety of locations from orbit by the GRS on the Mars Odyssey spacecraft (Keller *et al.* 2006) as well as in situ by every landed mission to date (Table 1). Chlorine concentrations determined from orbit by the GRS were for a 440–540 km diameter footprint in the top meter that occurred roughly between 45°S and 45°N latitude (Boynton *et al.* 2002; Keller *et al.* 2006). The Viking missions utilized XRF spectroscopy to examine scooped samples for total Cl (Clark *et al.* 1977). The Mars Pathfinder, Mars Exploration Rover and Mars Science Laboratory missions utilized APXS to determine *in situ* total chemistry including Cl of soil, sediment and rock (e.g. Rieder *et al.* 1997; Brückner *et al.* 2003; Rieder *et al.* 2004; Clark *et al.* 2005; Gellert *et al.* 2006; Morris *et al.* 2006; Ming *et al.* 2008; Blake *et al.* 2013; Gellert *et al.* 2013; Arvidson *et al.* 2014) (Table 1).

The fraction of oxychlorine relative to total chlorine can vary from site to site (10–95%) as is evident in the Phoenix and Gale data sets, which can make it difficult to ascertain what oxychlorine value to apply to a particular site with no oxychlorine measurements. However, knowledge of the type of material in which the oxychlorine was detected may provide constraints as to where a particular oxychlorine concentration can be applied elsewhere on Mars. The Rocknest eolian deposit in Gale Crater, for example, has eolian features (coarse-grained, indurated, bright dust-coated surface over darker finer sediment) and total chemistry similar to coarse-grained eolian deposits observed at both MER landing sites (Blake *et al.* 2013). The similarity of eolain materials between the MER and Gale landing sites could be argued as the result of global process that also leads to similar oxychlorine concentrations at in all soil and windblown sediments. The Rocknest oxychlorine component consists of ∼36% of total chlorine (Archer *et al.* 2015), which suggests that a similar fraction of oxychlorine-Cl may be present in the coarse-grained eolian deposits at the MER landing sites.

Oxychlorine species are likely to be globally distributed but the amount of oxychlorine as a percentage of total chlorine will likely vary from location to location. However, if two spatially different sites have materials with similar geologic properties (e.g. geochemistry, mineralogy, particle size distribution), then the oxychlorine/total Cl ratio of one site could potentially be used to constrain the oxychlorine concentration at the other site that has a known total Cl concentration.

Measurement challenges and alternative oxychlorine analytical techniques

The characterization of oxychlorine in martian sediments can be challenging because of the of low (<1 wt%) oxychlorine concentrations, difficulty in identifying the oxychlorine species present, and ensuring evolved O_2 as detected by EGA is attributed to oxychlorine. XRD and IR analysis detection limits for oxychlorine are >1 wt% and ∼>5–10 vol%, respectively. EGA while useful in detecting low oxychlorine concentrations (e.g. 0.1 wt% Table 1) can encounter difficulty in identifying which oxychlorine phases is present (e.g. chlorate versus perchlorate). The temperature in which O_2 is evolved can be used to identify which oxychlorine species is present; however, Fe phases in the sample can alter oxychlorine decomposition temperatures causing difficulties in identifying oxychlorine species. Furthermore, EGA of other gases, total chemistry (e.g. APXS), and/or XRD data may be required to rule out other non-oxychlorine sources of evolved O_2. The WCL ion-selective sensor has provided the only direct detection of oxychlorine as perchlorate in the martian soil. However, chlorate and nitrate could also have been present in the soil but were not detected because all three anions are only detectable by that ion-selective sensor. The presence of perchlorate in this case, inhibited the detection of the chlorate and nitrate. Future analysis of Mars soils or sediments with ion-selective sensors could continue to encounter this problem especially if lower concentrations of nitrate, perchlorate, and chlorate are present. The ion-selective sensor, in this case, would not be able to determine the proportion of perchlorate, chlorate and nitrate present in the sample. A potential solution to this problem would be to use an array of ISEs comprised of individual sensors where each possess different selectivity to the various oxy ions. For example, using 3 × 3 ISEs with ionophores of different selectivity for each of ClO_4^-, ClO_3^- and NO_3^- would then allow for use of a chemometric identification method of the individual responses and determination the respective concentrations.

The development of microfluidic devices also offers another suitable alternative for identifying and quantifying oxychlorine on future landed robotic missions to Mars. Several microchip based systems, which include isotachophoresis (ITP), ITP-capillary electrophoresis (ITP-CE), capillary electrophoresis (CE) and ion chromatography (IC) on a chip are being developed for terrestrial purposes (e.g. Evenhuis *et al.* 2004; Haddad *et al.* 2008). The reader is referred to the relevant literature for more detailed account of research and development of anion solution analysis using microchip technology (e.g. Murrihy *et al.* 2001; Evenhuis *et al.* 2004; Haddad *et al.* 2008). Briefly, the main purpose in developing this 'lab-on-a-chip'

https://doi.org/10.1017/S1473550416000057

technology for terrestrial needs is that less time, less sample and less reagents along with lower power requirements are required for analyses (Evenhuis *et al.* 2004). These attributes coupled with small instrument size are desirable for planetary instrumentation. The requirement of soil solution extracts for analysis can add a layer of complexity to overall instrument design that does not exist for IR, EGA and Chemin like XRD instruments. However, these microfluidic devices can detect much lower anion concentrations ($\sim$0.1 wt%) than IR and XRD techniques. Furthermore, microfluidic devices have the potential to more easily than EGA, to discriminate between chlorite (ClO_2^-), chlorate, and perchlorate phases without interferences from each other and other solution constituents (Evenhuis *et al.* 2004).

Summary

Chlorine was first detected on the surface of Mars by the Viking Landers at concentrations only found in arid environments on Earth. The species of Cl has long thought to be in chloride form (e.g. Clark & Baird, 1979). The Phoenix Lander's WCL analysis; however, yielded the surprising result that more than 86% of the soluble Cl consisted of perchlorate. The Phoenix Landers's TEGA instrument detected an evolved O_2 release from the Phoenix soil which supported the WCL perchlorate detection. The MSL rover's SAM instrument has also detected the presence of evolved O_2, HCl and chlorinated hydrocarbons consistent with the presence of perchlorate and/or chlorate salts. Further evaluation of the Viking GCMS data suggests that martian oxychlorine phases may have been detected in the Viking soils.

Perchlorate or chlorate salts have not been detected in Gale crater by CheMin. The lack of detection for oxychlorine phases could be attributed to several factors: (1) The oxychlorine phases could be poorly crystalline; (2) the oxychlorine abundance could be split between chlorate and perchlorate which drives the concentrations of these two species below the CheMin detection limits; and/or (3) the oxychlorine phases are at CheMin detection limits but are obscured by other basaltic phases present.

Orbital IR analysis has detected evidence consistent with the presence of hydrated perchlorate and chlorate in areas possessing RSL features. The co-occurrence of oxychlorine phases with Cl suggests that where ever Cl is detected the perchlorate or chlorate should be present. However, no evidence of perchlorate or chlorate has been observed especially in the anhydrous chloride enriched regions (up to 25 vol%) of Mars. Perhaps a physical/chemical mechanism may be operating that inhibits the formation or persistence of detectable oxychlorine in these chloride-rich regions.

Although the surface oxychlorine concentrations detected thus far by landed missions are below the orbital IR detection limits, a targeted search for oxychlorine phases in chloride rich regions may yield positive identification if abundances occur at the 5–10 vol% level. There are challenges in detecting oxychlorine phases by remote IR observations; however, oxychlorine/total Cl ratios obtained from the landed MSL and Phoenix missions has the potential to constrain oxychlorine levels at other locations where total Cl values have been or will be determined.

The development of microfluidic devices or 'lab-on-a-chip' technology may offer a suitable alternative for identifying and quantifying oxychlorine on future landed robotic missions to Mars. The small instrument size coupled with sensitivity to low anion concentrations, and the ability to identify individual oxychlorine species without interferences from other anions make microfluidic devices an attractive technology. Such instrumentation has the potential to make significant advancement in understanding the distribution and concentration of oxychlorine species and other soluble anions (e.g. nitrate, sulphate, phosphate, fluoride and chloride) on Mars.

Acknowledgements

We thank Deanne Rogers for processing the atmospherically corrected THEMIS scene used in this work (Fig. 6). This paper was written in response to the Perchlorate on Mars workshop (NASA Ames Research Center, Dec. 13–14, 2014). We thank the workshop organizers for bringing together leading perchlorate researchers to discuss this important topic that is relevant to Mars exploration. B.S., P.D.A, D.P.G., E.B.R. and D.W.M. gratefully acknowledge support from the Mars Science Laboratory mission. We are grateful to the anonymous reviewer who provided helpful comments that significantly improved this manuscript.

References

Acheson, R.J. & Jacobs, P.W.M. (1970). The thermal decomposition of magnesium perchlorate and of ammonium perchlorate and magnesium perchlorate mixtures. *J. Phys. Chem.* **74**, 281–288.

Archer, P.D., Jr. *et al.* (2014). Abundances and implications of volatile-bearing species from evolved gas analysis of the Rocknest aeolian deposit, Gale Crater, Mars. *J. Geophys. Res. Planet.* **119**, 237–254. DOI:10.1002/2013JE004493.

Archer, P.D. *et al.* (2015). Oxychlorine species on Mars: The Gale Crater Story. #2971. *46th Lunar Planet. Sci. Conf.*, March 16–20, The Woodlands, TX.

Arvidson, R.E. *et al.* (2014). Ancient aqueous environments at Endeavour Crater, Mars. *Science* **343**. DOI:10.1126/science.1248097.

Biemann, K. (1974). Test results on the Viking gas chromatograph–mass spectrometer experiment. *Orig. Life Evol. Biosph.* **5**, 417–430.

Biemann, K. (1979). The implications and limitations of the findings of the Viking organic analysis experiment. *J. Mol. Evol.* **14**, 65–70.

Biemann, K. & Bada, J.L. (2011). Comment on "Reanalysis of the Viking results suggests perchlorate and organics at midlatitudes on Mars" by Rafael Navarro-González *et al. J. Geophys. Res. Planet.* **116**, E12001. DOI:10.1029/2011JE003869.

Biemann, K., Oro, J., Toulmin, P., Orgel, L.E., Nier, A.O., Anderson, D.M. & Biller, J.A. (1976). Search for organic and volatile inorganic compounds in two surface samples from the Chryse Planitia region of Mars. *Science* **194**, 72–76.

Biemann, K. *et al.* (1977). The search for organic substances and inorganic volatile compounds in the surface of Mars. *J. Geophys. Res.* **82**, 4641–4658.

Bish, D.L. *et al.* (2013). X-ray diffraction results from Mars Science Laboratory: mineralogy of Rocknest at Gale Crater. *Science* **341**. DOI:10.1126/science.1238932.

Bishop, J.L., Quinn, R. & Dyar, M.D. (2014). What lurks in the martian rocks and soil? Investigations of sulfates, phosphates, and perchlorates spectral and thermal properties of perchlorate salts and implications for Mars. *Amer Miner* **99**, 1580–1592.

Blake, D.F. *et al*. (2012). Characterization and calibration of the CheMin mineralogical instrument on Mars Science Laboratory. *Space Sci. Rev*. **170**, 341–399.

Blake, D.F. *et al*. (2013). Curiosity at Gale Crater, Mars: characterization and analysis of the Rocknest sand shadow. *Science* **341**. DOI:10.1126/science.1239505.

Boynton, W.V. *et al*. (2002). Distribution of hydrogen in the near surface of Mars: evidence for subsurface ice deposits. *Science* **297**. DOI:10.1126/science.1073722.

Boynton, W.V. *et al*. (2009). Phoenix landing site evidence for calcium carbonate at the Mars. *Science* **325**, 61–64.

Brückner, J., Dreibus, G., Rieder, R. & Wänke, H. (2003). Refined data of the alpha proton X-ray spectrometer analyses of soils and rocks at the Mars Pathfinder site: implications for surface chemistry. *J. Geophys. Res. Planet*. **108**, 8094. doil:10.1029/2003JE002060.

Cannon, K.M., Sutter, B., Ming, D.W., Boynton, W.V. & Quinn, R. (2012). Perchlorate induced low temperature carbonate decomposition in the Mars Phoenix Thermal and Evolved Gas Analyzer (TEGA). *Geophys. Res. Lett*. **39**, L13203.

Catling, D.C., Claire, M.W., Zahnle, K.J., Quinn, R.C., Clark, B.C., Hecht, M.H. & Kounaves, S. (2010). Atmospheric origins of perchlorate on Mars and in the Atacama. *J. Geophys. Res*. **115**, E00E11. DOI:10.1029/2009JE003425.

Carrier, B.L. & Kounaves, S.P. (2015). The origins of perchlorate in the Martian soil. *Geophys. Res. Lett*. **42**, 3739–3745.

Chipera, S.J. & Bish, D.L. (2002). FULLPAT: a full pattern quantitative analysis program for X-ray powder diffraction using measured and calculated patterns. *J. Appl. Crystallogr*. **35**, 744–749.

Clark, B.C., Baird, A.K., Rose, H.J., Toulmin, P., Christian, R.P., Kelliher, W.C., Castro, A.J., Rowe, C.D., Keil, K. & Huss, G.R. (1977). The Viking X ray fluorescence experiment: Analytical methods and early results *J. Geophys. Res*. **82**, 4577–4594.

Clark, B.C. & Baird, A.K. (1979). Is the martian lithosphere sulfur rich? *J. Geophys. Res*. **84**, 8395–8403.

Clark, B.C., Baird, A.K., Weldon, R.J., Tsusaki, D.M., Schnable, L. & Candelaria, M.P. (1982). Chemical composition of martian fines. *J. Geophys. Res*. **87**, 10059–10067.

Clark, B.C. *et al*. (2005). Chemistry and mineralogy of outcrops at Meridiani Planum. *Earth Planet. Sci. Lett*. **240**, 73–94.

Cull, S.C., Arvidson, R.E., Catalano, J.G., Ming, D.W., Morris, R.V., Mellon, M.T. & Lemmon, M. (2010). Concentrated perchlorate at the Mars Phoenix landing site: evidence for thin film liquid water on Mars. *Geophys. Res. Lett*. **37**, L22203. DOI:10.1029/2010GL045269.

Evenhuis, C.J., Guijt, R.M., Macka, M., Haddad, P.R. (2004). Determination of inorganic anions using microfluidic devices. *Electrophoresis* **25**, 3602–3624.

Fang, D., Oberlin, E., Ding, W. & Kounaves, S.P. (2015). A common-factor approach for multivariate data cleaning with an application to Mars Phoenix mission data. ArXiv 2015. [cs.AI], 1510.01291.

Freissinet, C. *et al*. (2015). Organic molecules in the Sheepbed Mudstone, Gale Crater, Mars. *J. Geophys. Res. Planet*. **120**, 495–514. DOI:10.1002/2014JE004737.

Gellert, R. *et al*. (2006). Alpha particle X-ray spectrometer (APXS): results from Gusev crater and calibration report. *J. Geophys. Res*. **111**, E02S05. DOI:10.1029/2005JE002555.

Gellert, R. *et al*. (2013). Initial MSL APXS activities and observations at Gale Crater, Mars. 44th Lunar Planet. Sci. Conf., #1432, March 18–22, The Woodlands, TX.

Glavin, D.P. *et al*. (2013). Evidence for perchlorates and the origin of chlorinated hydrocarbons detected by SAM at the Rocknest aeolian deposit in Gale Crater. *J. Geophys. Res. Planet*. **118**, 1955–1973. DOI:10.1002/jgre.20144.

Glotch, T.D., Bandfield, J.L., Tornabene, L.L., Jensen, H.B. & Seelos, F.P. (2010). Distribution and formation of chlorides and phyllosilicates in Terra Sirenum, Mars. *Geophys. Res. Lett*. **37**, L16202. DOI:10.1029/2010GL044557.

Glotch, T.D., Bandfield, J.L., Wolff, M.J. & Arnold, J.A. (2013). Chloride salt deposits on Mars— No longer "putative." *44th Lunar Planet. Sci. Conf*., # 1549. March 18–22, The Woodlands, TX.

Glotch, T.D., Bandfield, J.L., Wolff, M.J., Arnold, J.A. & Che, C. (2016). Constraints on the composition and particle size of chloride salt-bearing deposits on Mars. *J. Geophys. Res. Planets*, **121**. DOI:10.1002/2015JE004921.

Goetz, W. *et al*. (2010). Microscopy analysis of soils at the Phoenix landing site, Mars: classification of soil particles and description of their optical and magnetic properties. *J. Geophys. Res. Planet*. **115**, E00E22. DOI:10.1029/2009JE003437.

Haddad, P.R., Nesterenko, P.N. & Buchberger, W. (2008). Recent developments and emerging directions in ion chromatography. *J. Chromatogr. A* **1184**, 456–473.

Hanley, J., Chevrier, V.F., Berget, D.J. & Adams, R.D. (2012). Chlorate salts and solutions on Mars. *Geophys. Res. Lett*. **39**, L08201. DOI:10.1029/2012GL051239.

Hanley, J., Chevrier, V.F., Barrows, S., Swaffer, C. & Altheide, T.S. (2015). Near- and mid-infrared reflectance spectra of hydrated oxychlorine salts with implications for Mars. *J. Geophys. Res. Planet* **120**, 1415–1426. DOI:10.1002/2013JE004575.

Hecht, M.H. *et al*. (2009). Detection of perchlorate and the soluble chemistry of martian soil at the Phoenix Lander Site. *Science* **325**, 64–67.

Hoffman, J.H., Chaney, R.C. & Hammack, H. (2008). Phoenix Mars mission – the thermal evolved gas analyzer. *J. Am. Soc. Mass Spectrom*. **19**, 1377–1383.

Jackson, W.A. *et al*. (2015). Global patterns and environmental controls of perchlorate and nitrate co-occurrence in arid and semi-arid environments. *Geochim. Cosmochim. Acta* **164**, 502–522.

Jensen, H.B. & Glotch, T.D. (2011). Investigation of the near-infrared spectral character of putative Martian chloride deposits. *J. Geophys. Res*. **116**, E00J03. DOI:10.1029/2011JE003887.

Keller, J.M. *et al*. (2006). Equatorial and midlatitude distribution of chlorine measured by Mars Odyssey GRS. *J. Geophys. Res*. **111**, E03S08. DOI:10.1029/2006JE002679.

Kounaves, S.P. *et al*. (2009). The MECA wet chemistry laboratory on the 2007 phoenix mars Scout lander. *J. Geophys. Res*. **114**, E00A19. DOI:10.1029/2008JE003084.

Kounaves, S.P. *et al*. (2010). Wet chemistry experiments on the 2007 Phoenix Mars Scout Lander mission: data analysis and results. *J. Geophys. Res. Planet*. **115**, E00E10. DOI:10.1029/2009JE003424.

Kounaves, S.P., Nikos, A., Chaniotakis, N.A., Chevrier, V.F., Carrier, B.L., Folds, K.E., Hansen, V.M., McElhoney, K.M., O'Neil, G.D. & Weber, A. W. (2014a). Identification of the perchlorate parent salts at the Phoenix Mars landing site and possible implications. *Icarus* **232**, 226–231.

Kounaves, S.P., Carrier, B.L., O'Neil, G.D., Stroble, S.T. & Claire, M.W. (2014b). Evidence of martian perchlorate, chlorate, and nitrate in Mars meteorite EETA79001: implications for oxidants and organics. *Icarus* **229**, 206–213.

Lauer, H.V., Ming, D.W., Sutter, B., Golden, D.C., Morris, R.V. & Boynton, W.V. (2009). Thermal and evolved gas analysis of magnesium perchlorate: Implications for perchlorates in soils at the Mars Phoenix Landing site. *40th Lunar Planet. Sci. Conf*. #2196, March 23–27, 2009, The Woodlands, TX.

Lee, J.S. & Hsu, C.K. (2001). The DSC studies on the phase transition, decomposition and melting of potassium perchlorate with additives. *Thermochim. Acta* **367–368**, 367–370.

Leshin, L.A. *et al*. (2013). Volatile, isotope, and organic analysis of martian fines with the Mars Curiosity Rover. *Science* **341**, 1238937–1–9.

Mahaffy, P.R. *et al*. (2012). The sample analysis at Mars investigation and instrument suite. *Space Sci. Rev*. **170**, 401–478.

Marion, G.M., Catling, D.C., Zahnle, K.J. & Claire, M.W. (2010). Modeling aqeous perchlorate chemistries with applications to Mars. *Icarus* **207**, 675–685.

Markowitz, M.M. (1963). A basis for the prediction of the thermal decomposition products of metal perchlorates. *J. Inorg. Nucl. Chem*. **25**, 407–414.

Marvin, G.G. & Woolaver, L.B. (1945). Thermal decomposition of perchlorates. *Indust. Eng. Chem*. **17**, 474–476.

McAdam, A.C. *et al*. (2014). Sulfur-bearing phases detected by evolved gas analysis of the Rocknest aeolian deposit, Gale Crater, Mars. *J. Geophys. Res. Planet*. **119**, 373–393.

Migdal-Mikuli, A. & Hetmańczyk, J. (2008). Thermal behavior of $[Ca(H_2O)_4](ClO_4)_2$ and $[Ca(NH_3)_6](ClO_4)_2$. *J. Therm. Anal. Calor*. **91**, 529–534.

Miller, F.A. & Wilkins, C.H. (1952). Infrared spectra and characteristic frequencies of inorganic ions. *Anal. Chem*. **24**, 1253–1294.

Ming, D.W. *et al*. (2008). Geochemical properties of rocks and soils in Gusev Crater, Mars: results of the alpha particle X-ray spectrometer from Cumberland Ridge to home plate. *J. Geophys. Res*. **113**, E12S39. DOI:10.1029/2008JE003195.

Ming, D.W. *et al*. (2014). Volatile and organic compositions of sedimentary rocks in Yellowknife Bay, Gale Crater, Mars. *Science* **343**, 1245267. http://doi.org/10.1126/science.1245267.

Morris, R.V. *et al*. (2006). Mössbauer mineralogy of rock, soil, and dust at Meridiani Planum, Mars: opportunity's journey across sulfate-rich outcrop, basaltic sand and dust, and hematite lag deposits. *J. Geophys. Res*. **111**, E12S15. DOI:10.1029/2006JE002791.

Morris, R.V., Golden, D.C., Ming, D.W., Graff, T.G., Arvidson, R.E., Wiseman, S.M., Lichtenberg, K.A. & Cull, S. (2009). Visible and near-IR reflectance spectra for smectite, sulfate, and perchlorate under dry conditions for interpretation of martian surface mineralogy. *40*th *Lunar Planet. Sci. Conf*. #2317, March 23–27, The Woodlands, TX.

Murchie, S.L. *et al*. (2009). A synthesis of Martian aqueous mineralogy after 1 Mars year of observations from the Mars Reconnaissance Orbiter. *J. Geophys. Res*. **114**, E00D06. DOI:10.1029/2009JE003342.

Murrihy, J.P. *et al*. (2001). Ion chromatography on-chip. *J. Chromatography A* **924**, 233–238.

Navarro-González, R. & McKay, C.P. (2011). Reply to comment by Biemann and Bada on "Reanalysis of the Viking results suggests perchlorate and organics at midlatitudes on Mars," *J. Geophys. Res. Planet*. **116**, E12002. DOI:10.1029/2011JE003880.

Navarro-González, R., Vargas, E., de la Rosa, J., Raga, A.C. & McKay, C.P. (2010). Reanalysis of the Viking results suggests perchlorate and organics at midlatitudes on Mars. *J. Geophys. Res. Planet*. **115**, E12010. DOI:10.1029/2010JE003599.

Ojha, L., Wilhelm, M.B., Murchie, S.L., McEwen, A.S., Wray, J.L., Hanley, J., Massé, M. & Chojnacki, M. (2015). Spectral evidence for hydrated salts in recurring slope lineae on Mars. *Nat. Geosci*. **8**, 829–832.

Osterloo, M.M., Hamilton, V.E., Bandfield, J.L., Glotch, T.D., Baldridge, A.M., Christensen, P.R., Tornabene, L.L. & Anderson, F.S. (2008). Chloride-bearing materials in the southern highlands of Mars. *Science* **319**, 1651–1654.

Osterloo, M.M., Anderson, F.S., Hamilton, V.E. & Hynek, B.M. (2010). Geologic context of proposed chloride bearing materials on Mars. *J. Geophys. Res*. **115**, E10012. DOI:10.1029/2010JE003613.

Pejov, L. & Petruševski, V. (2002). Fourier transform infrared study of perchlorate ($^{35}ClO_4^-$ and $^{37}ClO_4^-$) anions isomorphously isolated in potassium permanganate matrix. Vibrational anharmonicity and pseudo-symmetry effects. *J. Phys. Chem. Sol*. **63**, 2873–1881.

Rampe, E.B., Morris, R.V., Ruff, S.W., Horgan, B., Dehouck, E., Achilles, C.N., Ming, D.W., Bish, D.L., Chipera, S.J. & the MSL Science Team. (2014). Amorphous phases on the surface of Mars. *Eighth International Conference on Mars*, #1239, Pasadena, CA.

Rao, B., Hatzinger, P.B., Bohlke, J.K., Sturchio, N.C., Eckardt, F.D. & Jackson, W.A. (2010). Natural chlorate in the environment: application of a new IC-ESI/MS/MS method with a Cl18O3-internal standard. *Environ. Sci. Technol*. **44**, 8429–8434.

Rieder, R., Economou, T., Wanke, H., Turkevich, A., Crisp, J., Brückner, J., Dreibus, G. & McSween, H.Y. (1997). The chemical composition of martian soil and rocks returned by the mobile alpha proton X-ray spectrometer: preliminary results from the x-ray mode. *Science* **278**, 1771–1774.

Rieder, R. *et al*. (2004). Chemistry of rocks and soils at Meridiani Planum from the Alpha Particle X-ray Spectrometer. *Science* **306**, 1746–1749.

Robertson, K. & Bish, D. (2011). Stability of phases in the $Mg(ClO_4)_2{\cdot}nH_2O$ system and implications for perchlorate occurrences on Mars. *J. Geophys. Res. Planet*. **116**, E07006. DOI:10.1029/2010JE003754.

Ruesch, O., Poulet, F., Vincendon, M., Bibring, J.-P., Carter, J., Erkeling, G., Gondet, B., Hiesinger, H., Ody, A. & Reiss, D. (2012). Compositional investigation of the proposed chloride-bearing materials on Mars using near-infrared orbital data from OMEGA/MEx. *J. Geophys. Res*. **117**, E00J13. DOI:10.1029/2012JE004108.

Rudloff, W.K. & Freeman, E.S. (1970). Catalytic effect of metal oxides on thermal decomposition reactions. II. The catalytic effect of metal oxides on the thermal decomposition of potassium chlorate and potassium perchlorate as detected by thermal analysis methods. *J. Phys. Chem*. **74**, 3317–3324.

Ruff, S.W., Christensen, P.R., Barbera, P.W. & Anderson, D.L. (1997). Quantitative thermal emission spectroscopy of minerals: a laboratory technique for measurement and calibration. *J. Geophys. Res*. **102**, 14899–14913. DOI:10.1029/97JB00593.

Rushneck, D.R., Diaz, A.V., Howarth, D.W., Rampacek, J., Olson, K.W., Dencker, W.D., Smith, P., McDavid, L., Tomassian, A., Harris, M., Bulota, K., Biemann, K., LaFleur, A.L., Biller, J.E., Owen, T. (1978). Viking gas chromatograph–mass spectrometer. *Rev. Sci. Instrum*. **49**, 817–834. http://doi.org/doi:10.1063/1.1135623

Seelos, K.D. *et al*. (2008). Geomorphologic and mineralogic characterization of the northern plains of Mars at the Phoenix Mission candidate landing sites. *J. Geophys. Res. Planet*. **113**, E00A13. DOI:10.1029/2008JE003088.

Smith, P.H. *et al*. (2009). H_2O at the Phoenix landing site. *Science* **325**, 58–61.

Stern, J.C. *et al*. (2015). Evidence for indigenous nitrogen in sedimentary and aeolian deposits from the Curiosity rover investigations at Gale Crate, Mars. *Proc. Natl. Acad. Sci. U.S.A*. **112**, 4254–4250.

Sutter, B., Dalton, J.B., Ewing, S.A., Amundson, R. & McKay, C.P. (2007). Terrestrial analogs for interpretation of infrared spectra from the martian surface and subsurface: sulfate, nitrate, carbonate, and phyllosilicate-bearing Atacama Desert soils. *J. Geophys. Res*. **112**, G04S10. DOI:10.1029/2006JG000313.

Toner, J.D., Catling, D.C. & Light, B. (2014). Soluble salts at the Phoenix Lander site, Mars: a reanalysis of the Wet Chemistry Laboratory data. *Geochim. Cosmochim. Acta* **136**, 142–168.

Vaniman, D.T. *et al*. (2014). Mineralogy of a mudstone at Yellowknife Bay, Gale Crater, Mars. *Science* **343**. 10.1126/science.1243480.

Wray, J.J., Murchie, S.L., Squyres, S.W., Seelos, F.P. & Tornabene, L.L. (2009). Diverse aqueous environments on ancient Mars revealed in the southern highlands. *Geology* **37**, 1043–1046.

Wu, S.-H., Chi, J.-H., Huang, C.-C., Lin, N.-K., Peng, J.-J. & Shu, C.-M. (2010). Thermal hazard analyses and incompatible reaction evaluation of hydrogen peroxide by DSC. *J. Therm. Anal. Calorim*. **102**, 563–568.

Yen, A.S. *et al*. (2006). Nickel on Mars: constraints on meteoritic material at the surface. *J. Geophys. Res*. **111**, E12S11. DOI:10.1029/2006JE002797.

Young, R.A. (1993). Introduction to the Rietveld method. In *The Rietveld Method, Intl Union Crystallography Monographs Crystallography*, vol. **5**, ed. Young, R.A., pp. 1–38. Oxford University Press, Oxford, UK.

Zent, A.P. & McKay, C.P. (1994). The chemical reactivity of the martian soil and implications for future missions. *Icarus* **108**, 146–157.